scientific reports

Check for updates

OPEN

Pd-containing magnetic periodic mesoporous organosilica nanocomposite as an efficient and highly recoverable catalyst

Maryam Neysi & Dawood Elhamifar✉

A novel magnetic ionic liquid based periodic mesoporous organosilica supported palladium (Fe_3O_4@SiO_2@IL-PMO/Pd) nanocomposite is synthesized, characterized and its catalytic performance is investigated in the Heck reaction. The Fe_3O_4@SiO_2@IL-PMO/Pd nanocatalyst was characterized using FT-IR, PXRD, SEM, TEM, VSM, TG, nitrogen-sorption and EDX analyses. This nanocomposite was effectively employed as catalyst in the Heck reaction to give corresponding arylalkenes in high yield. The recovery test was performed to study the catalyst stability and durability under applied conditions.

In recent years, magnetite nanoparticles, due to their magnetic properties, biocompatibility and easy separation have received a great deal of attention in various fields of science and technology. These have a lot of applications in the areas of catalysis, sensors, drug delivery, water purification and separation[1–6]. However, if the surface of these NPs is left untreated, they oxidize easily and large clusters are formed by the agglomeration of small Fe_3O_4 NPs that limit their use for practical applications. To overcome these problems, various shell/covers such as noble metals, metal oxide, silica and polymers have been employed for the protection of magnetite NPs[5,7–14]. Among these, silica shells due to their high chemical stability, versatility for surface modification and great biocompatibility are known to be one of the most suitable coating layers. Hence, silica-coated MNPs provide a vast perspective for designing efficient magnetic catalyst supports[14–19]. On the other hand, periodic mesoporous organosilica (PMOs) are a desirable class of organic–inorganic materials that have emerged as an ideal shell for MNPs, due to their excellent properties such as high surface area, high lipophilicity and high thermal and mechanical stability[20–23]. Some recently reported magnetic catalytic systems include Fe_3O_4@SiO_2/Pr-*N* = Mo[Mo_5O_{18}][24], Fe_3O_4@SiO_2@HPG-$OPPh_2$-PNP[25], Fe_3O_4@SiO_2[14], Fe_3O_4@SiO_2/Shiff-base/M[26], Fe_3O_4@nSiO_2@mSiO_2[27] and Fe_3O_4@SiO_2@TiO_2[28].

Ionic liquids (ILs), due to their ability to dissolve a diversity of compounds, have attracted tremendous attention in chemistry and material sciences in the last decade[29–31]. In particular, recently imidazolium-based ILs have been widely used as an outstanding stabilizer for metal nanoparticles during catalytic reactions; also, as a linker that connects catalyst to solid-supports which further enhance the catalytic activity[32–34]. Some of newly developed systems are, Fe_3O_4/KCC-1/IL/HPW[35]. Fe_3O_4@SiO_2@$(CH_2)_3$-imidazole-SO_3H[36], L-proline-IL-SiO_2@Fe_3O_4[34], Fe_3O_4@nSiO_2@mSiO_2/Pr-Imi-NH_2.Ag[33] and Fe_3O_4@SiO_2@MIPs[32].

The Heck coupling reaction is one of the most important organic reaction involving Pd-catalyzed coupling of aryl halides and olefins in the presence of a base. Some of the magnetic catalysts that have been used for the Heck reaction are Fe_3O_4@DAG/Pd[37], Fe_3O_4@SiO_2@Carbapalladacycle[38], Fe_3O_4@SiO_2–imid–PMA[39], Fe_3O_4@PAA-Pd(II)[40] and Pd/-AlOOH@Fe_3O_4[41].

In view of the above, in this study, a novel Pd-containing magnetic IL-based PMO (Fe_3O_4@SiO_2@IL-PMO/Pd) is prepared, characterized and its catalytic application is investigated in the Heck reaction.

Experimental section

Preparation of Fe_3O_4@SiO_2@IL-PMO nanoparticles. First, the Fe_3O_4@SiO_2 NPs were prepared according to a previous report[42]. In order to prepare Fe_3O_4@SiO_2@IL-PMO, 0.5 g of Fe_3O_4@SiO_2 was added to a flask containing distilled water (5 mL), HCl (2 M, 11 mL) and KCl (3 g) while stirring at 40 °C. Then, 1.5 g of pluronic P123 was added and stirring was continued at 40 °C for 3 h. Next, 0.2 g of 1,3-bis(trimethoxysilylpropyl) imidazolium chloride and 1.5 mL of tetramethoxysilane (TMOS) were added and the resulted mixture was

Department of Chemistry, Yasouj University, Yasouj 75918-74831, Iran. ✉email: d.elhamifar@yu.ac.ir

stirred at 25 °C for 24 h under an argon atmosphere. The resulted combination was aged for 72 h at 100 °C. After that, the product was separated using an external magnet, washed with water and EtOH and dried at 70 °C for 12 h[43]. The P123 surfactant was removed by a Soxhlet apparatus using acidic ethanol. The final material was called Fe_3O_4@SiO_2@IL-PMO.

Preparation of Fe_3O_4@SiO_2@IL-PMO/Pd. For this, 0.25 g of Fe_3O_4@SiO_2@IL-PMO was completely dispersed in 40 mL of dimethyl sulfoxide (DMSO) under ultrasonic irradiation for 20 min. Then, 0.025 g of Pd $(OAc)_2\cdot 4H_2O$ was added and the obtained mixture was stirred at 25 °C for 24 h. Next, the product was separated using a magnet, washed, dried at 70 °C and called Fe_3O_4@SiO_2@IL-PMO/Pd.

Procedure for Heck coupling using Fe_3O_4@SiO_2@IL-PMO/Pd nanocatalyst. For this purpose, 0.48 mol% of Fe_3O_4@SiO_2@IL-PMO/Pd was added to a DMF solution of Ar-X (1 mmol), alkyl acrylate (2 mmol) and base (2 mmol). This was stirred at 105 °C. After completion of the reaction, ethyl acetate (10 mL) and water (10 mL) were added and the catalyst was separated by a magnet. The mixture was decanted and the organic phase was separated and dried over Na_2SO_4. The desired products were obtained after evaporation of solvent and/or recrystallization.

Results and discussion

The Fe_3O_4@SiO_2@IL-PMO/Pd nanocomposite was prepared according to Fig. 1. As shown, Fe_3O_4@SiO_2 was first prepared by coating a silica layer over the Fe_3O_4 surface. Then, the IL-PMO shell was created over Fe_3O_4@SiO_2 via hydrolysis and co-condensation of TMOS and ionic liquid in the presence of pluronic p123 template. The Fe_3O_4@SiO_2@IL-PMO/Pd nanocomposite was finally obtained via treatment of Fe_3O_4@SiO_2@IL-PMO with $Pd(OAc)_2$.

Figure 2 shows the FT-IR spectra of prepared materials. For all samples, the bands appeared at 586 and 3400 cm^{-1} are, respectively, assigned to Fe–O and O–H bonds (Fig. 2). For the Fe_3O_4@SiO_2 and Fe_3O_4@SiO_2@IL-PMO/Pd materials, the peaks at 823 and 1077 cm^{-1} are assigned to Si–O–Si bands indicating successful coating of amorphous silica on Fe_3O_4 (Fig. 2b). Moreover, for the Fe_3O_4@SiO_2@IL-PMO/Pd material, the peaks appeared at 2923, 1420, and 1625 cm^{-1} are, respectively, due to the vibrations of aliphatic C–H, C=C and C=N bands of IL rings (Fig. 2c). These results confirm the successful coating of silica and IL-based periodic mesoporous organosilica shells over magnetite NPs.

Figure 3 shows the wide-angle PXRD analysis of Fe_3O_4, Fe_3O_4@SiO_2, Fe_3O_4@SiO_2@IL-PMO and Fe_3O_4@SiO_2@IL-PMO/Pd nanoparticles. The signals at 30.3, 35.7, 43.4, 53.8, 57.7 and 63.0 are, respectively, due to the reflections of 220, 311, 400, 422, 511 and 440. This confirms high stability of crystalline structure of magnetite NPs during catalyst preparation. It is also important to note that, for Fe_3O_4@SiO_2, Fe_3O_4@SiO_2@IL-PMO and Fe_3O_4@SiO_2@IL-PMO/Pd materials, the intensity of PXRD peaks is decreased, indicating the successful modification of magnetite NPs with SiO_2, IL-PMO and palladium moieties.

The low-angle PXRD analysis of the Fe_3O_4@SiO_2@IL-PMO/Pd nanocomposite demonstrated a sharp peak at $2\theta \approx 1$ corresponding to the IL-PMO shell (Fig. 4).

The N_2 adsorption–desorption isotherm of the Fe_3O_4@SiO_2@IL-PMO/Pd showed a type IV isotherm with a H1 hysteresis loop, which is characteristic of ordered mesostructures with high regularity (Fig. 5). Also, the BET surface area, average pore size and total pore volume of the designed Fe_3O_4@SiO_2@IL-PMO/Pd nanocomposite were found to be 496.29 m^2/g, 4.64 nm and 0.76 cm^3/g, respectively. These results are in good agreement with low-angle PXRD analysis proving well formation of an ordered PMO shell for Fe_3O_4@SiO_2@IL-PMO/Pd.

The VSM analysis was performed to investigate the magnetic properties of Fe_3O_4@SiO_2@IL-PMO/Pd (Fig. 6). This showed a saturation magnetization about 45 $emu\cdot g^{-1}$, which is lower than that of pure magnetic iron oxide NPs (60 emu g^{-1})[44]. This proves the successful coating of SiO_2 and PMO shells over magnetite NPs and also confirms the high magnetic properties of the catalyst which is an excellent characteristic in the catalytic fields.

The EDX pattern of Fe_3O_4@SiO_2@IL-PMO/Pd demonstrated the signals of Fe, O, Si, C, Cl, Pd and N elements, conforming successful coating/immobilization of SiO_2, ionic liquid and Pd moieties on magnetite NPs (Fig. 7).

The SEM analysis of Fe_3O_4, Fe_3O_4@SiO_2, Fe_3O_4@SiO_2@IL-PMO and Fe_3O_4@SiO_2@IL-PMO/Pd showed a uniform spherical morphology for all samples (Fig. 8). Furthermore, according to the histogram of the SEM images (Fig. 9, inset), the average particle size of Fe_3O_4, Fe_3O_4@SiO_2, Fe_3O_4@SiO_2@IL-PMO and Fe_3O_4@SiO_2@IL-PMO/Pd NPs were 20.00 ± 2.10, 30.11 ± 2.12, 49.20 ± 2.30 and 51.22 ± 2.42 nm, respectively. The increase in the particle size after each step confirms the successful shell formation and modification of magnetite NPs according to Fig. 1.

The TEM image of Fe_3O_4@SiO_2@IL-PMO/Pd material also showed spherical particles with a black core (magnetite NPs) and gray shell (SiO_2@IL-PMO layer) (Fig. 9).

According to TG analysis, a weight loss of about 9% was observed corresponding to the immobilized/incorporated ionic liquid groups onto/into material framework (Fig. 10).

The Heck reaction was selected as a valuable coupling reaction to evaluate the catalytic activity of Fe_3O_4@SiO_2@IL-PMO/Pd as a heterogeneous catalyst. The Heck reaction between iodobenzene and ethyl acrylate was selected as a test model. The effect of solvent showed that DMF is the best giving an excellent yield of 98% (Table 1, entries 1–5). The study also showed that the rate of reaction is affected by the amount of the catalyst. As shown, the reaction yield is increased with increasing catalyst loading from 0.24 to 0.48 mol% (Table 1, entry 5 *vs* entry 6). Among various bases, K_2CO_3 was the most effective compared to others (Table 1, entry 5 *vs* entries 8–11). Screening different temperatures showed that at 105 °C the best result is delivered (Table 1, entry 5 *vs* entries 12, 13). Accordingly, the use of 0.48 mol% of Fe_3O_4@SiO_2@IL-PMO/Pd and DMF at 105 ºC were selected as optimum conditions. In the next study, this Heck reaction was performed using Pd-free Fe_3O_4@SiO_2@IL-PMO and Fe_3O_4@SiO_2 materials under the same conditions as Fe_3O_4@SiO_2@IL-PMO/Pd. Interestingly, in the

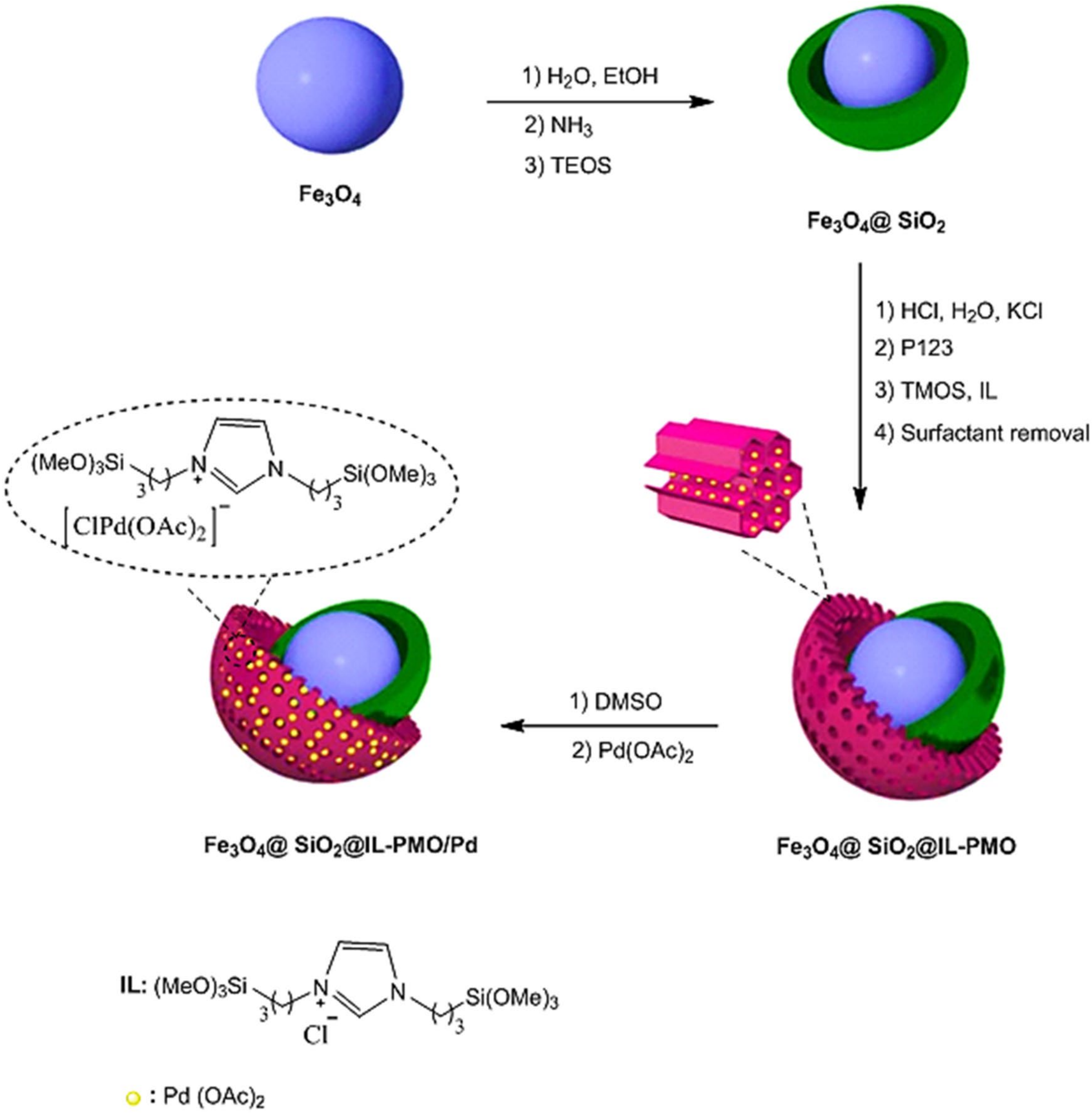

Figure 1. Preparation of $Fe_3O_4@SiO_2@IL\text{-}PMO/Pd$.

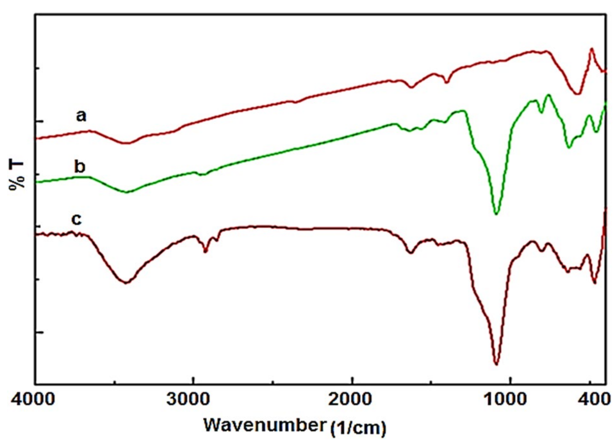

Figure 2. FT-IR spectra of (**a**) Fe_3O_4, (**b**) $Fe_3O_4@SiO_2$ and (**c**) $Fe_3O_4@SiO_2@IL\text{-}PMO/Pd$ materials.

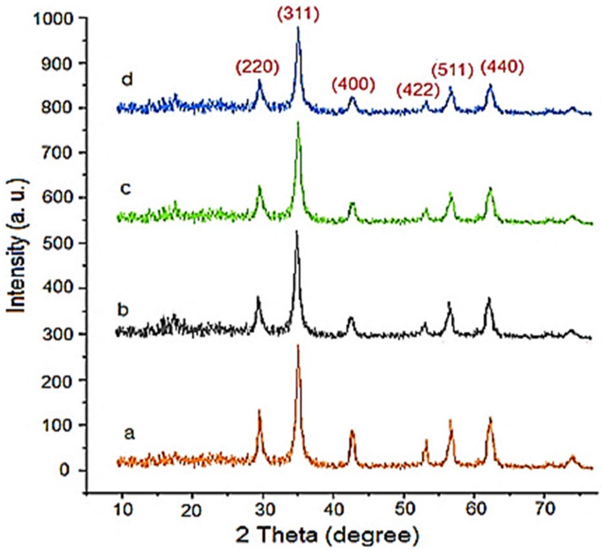

Figure 3. (**a**) Wide-angle PXRD of (**a**) Fe_3O_4, (**b**) Fe_3O_4@SiO_2, (**c**) Fe_3O_4@SiO_2@IL-PMO and (**d**) Fe_3O_4@SiO_2@IL-PMO/Pd.

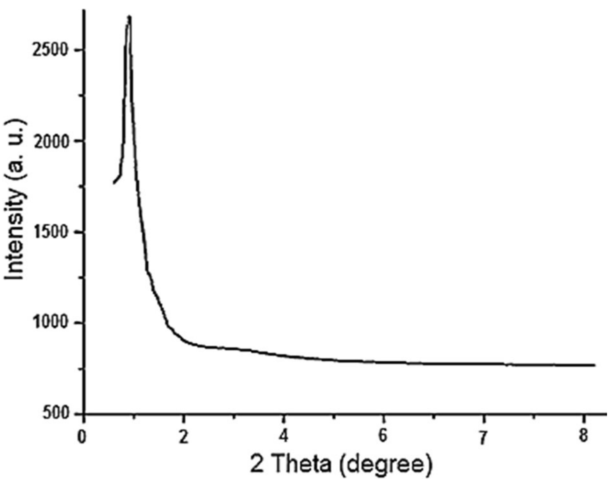

Figure 4. Low-angle PXRD patterns of Fe_3O_4@SiO_2@IL-PMO/Pd.

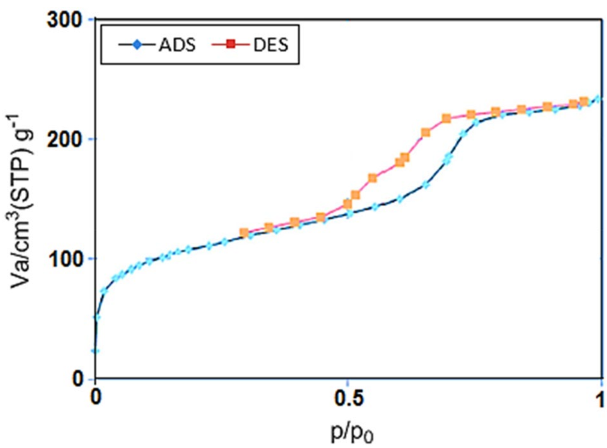

Figure 5. N_2 adsorption–desorption isotherm of Fe_3O_4@SiO_2@IL-PMO/Pd.

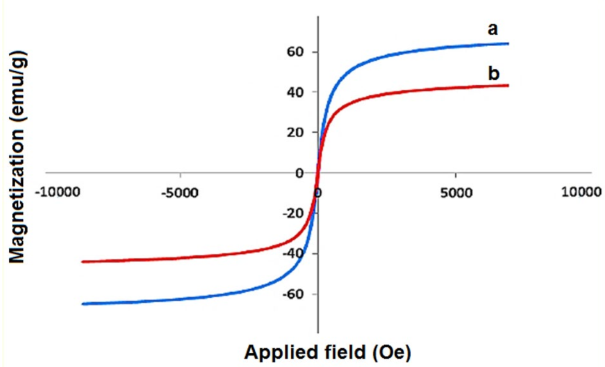

Figure 6. VSM analysis of the (**a**) Fe_3O_4 and (**b**) Fe_3O_4@ SiO_2@IL-PMO/Pd.

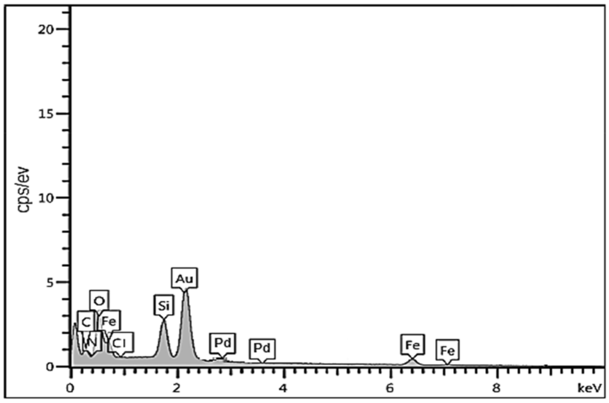

Figure 7. EDX analysis of Fe_3O_4@SiO_2@IL-PMO/Pd.

latter study no conversion was observed indicating that the process is actually catalyzed by supported Pd species (Table 1, entry 5 *vs* entries 14, 15).

After optimization, the catalyst was employed in the Heck-coupling reaction for the preparation of some styrene derivatives. As shown in Table 2, all aryl halides bearing both electron-withdrawing and electron-donating substituents reacted effectively with acrylates to give corresponding Heck products in high yield. This demonstrates high efficiency of Fe_3O_4@SiO_2@IL-PMO/Pd nanocomposite for the preparation of a wide-range of important arylalkenes.

The recovery of Fe_3O_4@SiO_2@IL-PMO/Pd was also investigated under optimum conditions. For this, after each reaction cycle, the catalyst was removed magnetically and after washing and drying, it was reused in the next run. The results showed that the catalyst could be recovered and reused for four times with no important reduction in its performance (Fig. 11).

Conclusion

In this study, a novel core–shell structured Fe_3O_4@SiO_2@IL-PMO/Pd nanocomposite was synthesized and characterized. The well immobilization/incorporation and high stability of ionic liquid and palladium moieties over magnetite NPs were confirmed by FT-IR, TG and EDX analyses. The VSM and PXRD showed good magnetic properties of Fe_3O_4@SiO_2@IL-PMO/Pd. The nitrogen-sorption and low-angle PXRD showed a mesoporous shell for the designed material. This nanocomposite was catalytically employed in the Heck reaction giving high yield of corresponding coupling products. The recovery test demonstrated high stability and durability of active catalytic species during applied conditions.

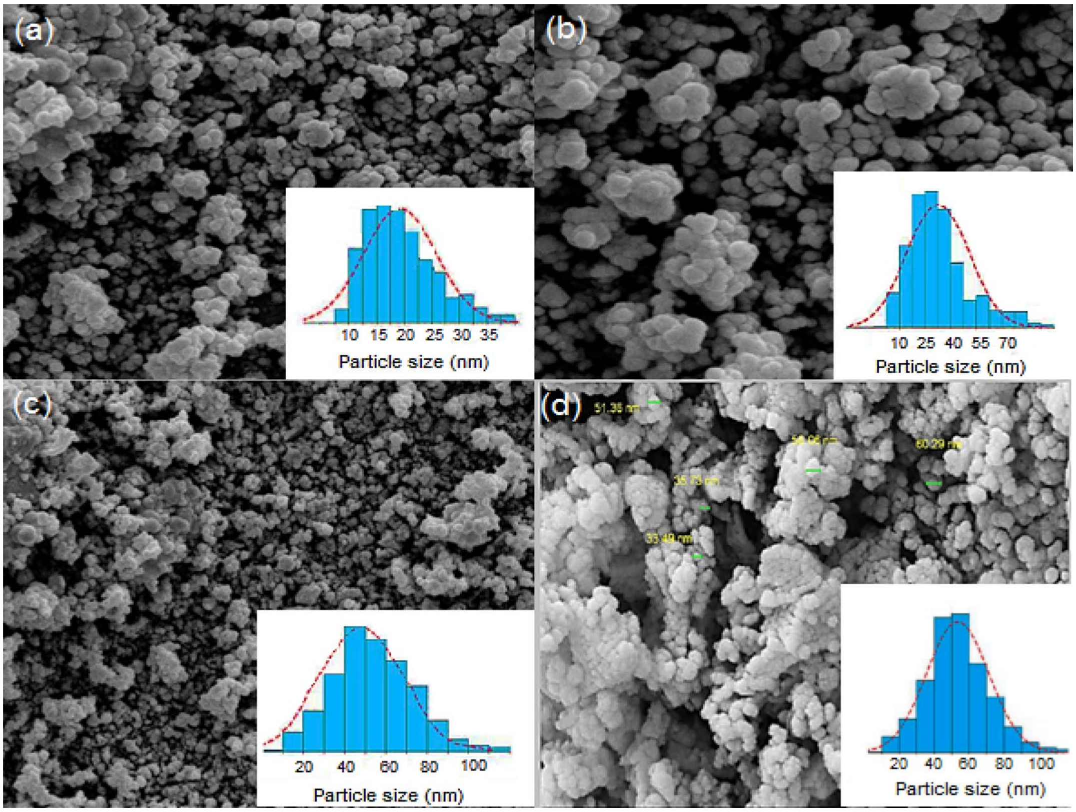

Figure 8. SEM image of (**a**) Fe_3O_4, (**b**) Fe_3O_4@SiO_2, (**c**) Fe_3O_4@SiO_2@IL-PMO and (**d**) Fe_3O_4@SiO_2@IL-PMO/Pd materials.

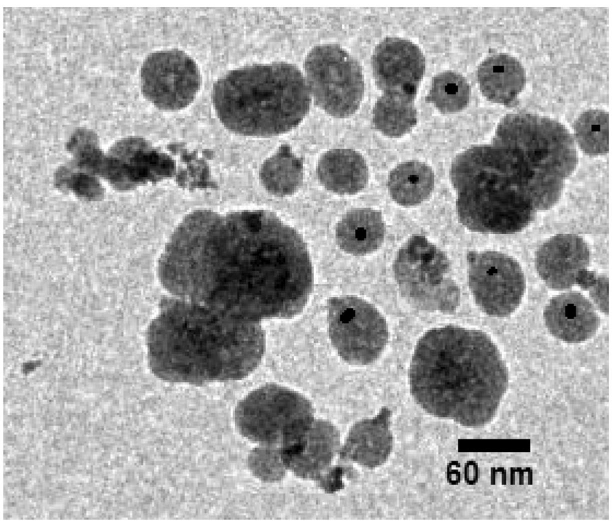

Figure 9. TEM image of Fe_3O_4@SiO_2@IL-PMO/Pd.

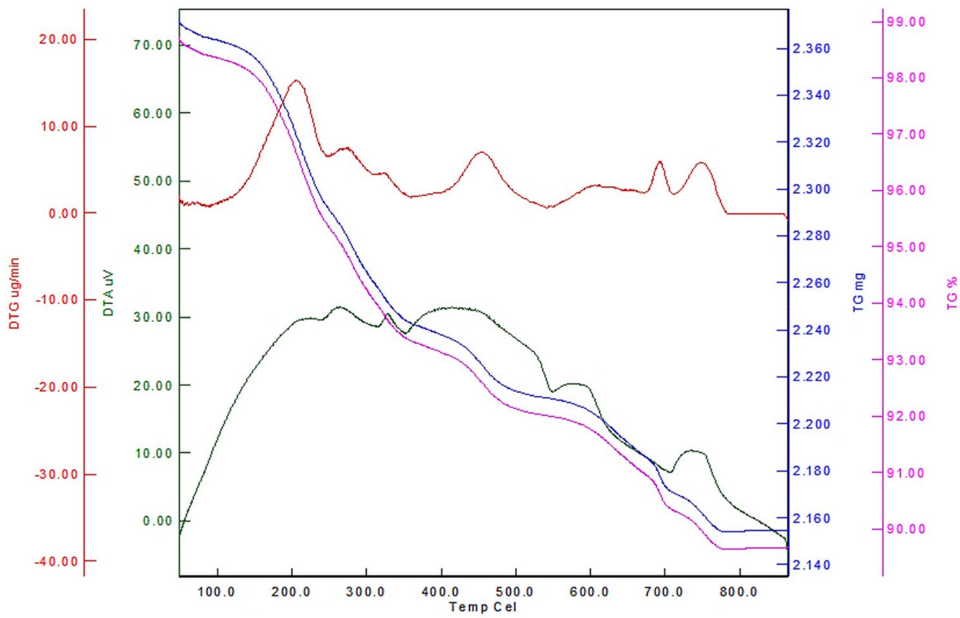

Figure 10. The TG analysis of Fe_3O_4@SiO_2@IL-PMO/Pd.

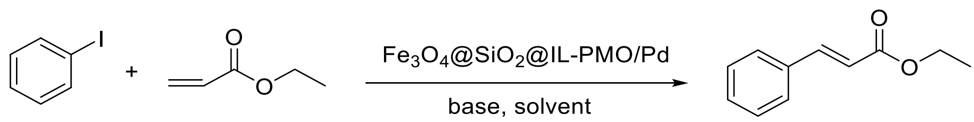

Entry	Solvent	Base	Catalyst (mol%)	T (°C)	Yield (%)
1	EtOH	K_2CO_3	0.48	105	35
2	CH3CN	K_2CO_3	0.48	105	60
3	Toluene	K_2CO_3	0.48	105	65
4	NMP	K_2CO_3	0.48	105	85
5	DMF	K_2CO_3	0.48	105	98
6	DMF	K_2CO_3	0.24	105	85
7	DMF	K_2CO_3	0.97	105	98
8	DMF	NEt_3	0.48	105	88
9	DMF	K_3PO_4	0.48	105	60
10	DMF	NaOAc	0.48	105	76
11	DMF	NaOH	0.48	105	55
12	DMF	K_2CO_3	0.48	85	20
13	DMF	K_2CO_3	0.48	120	98
14	DMF	K_2CO_3	Fe_3O_4@SiO_2@ IL-PMO (0.004 g)	105	N. R.
15	DMF	K_2CO_3	Fe_3O_4@ SiO_2 (0.004 g)	105	N. R.

Table 1. Screening different parameters in the Heck reaction.

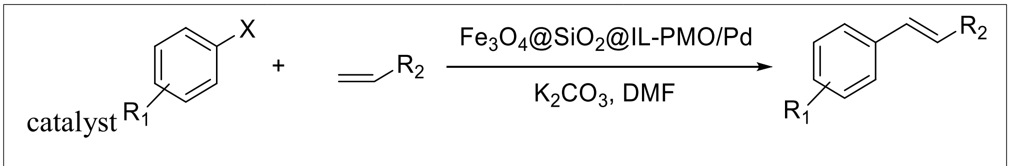

Entry	X	R_1	R_2	Time	Yield (%)
1	I	H	CO_2Et	30 min	98
2	I	H	CO_2Me	30 min	98
3	I	H	CO_2Bu	40 min	96
4	Br	H	CO_2Et	2 h	95
5	Br	H	CO_2Me	2 h	97
6	Br	H	CO_2Bu	2.5 h	95
7	Br	4-MeO	CO_2Me	10 h	90
8	Cl	4-MeO	CO_2Me	17 h	85
9	Br	4-NO_2	CO_2Me	7 h	96
10	Cl	4-CHO	CO_2Bu	12 h	89

Table 2. Heck reaction of aryl halides and acrylates using $Fe_3O_4@SiO_2@IL-PMO/Pd$ catalyst.

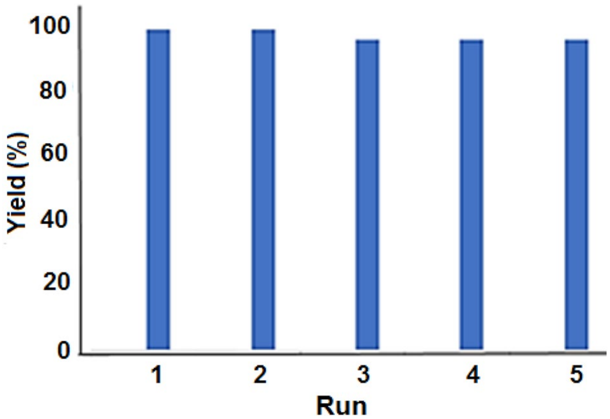

Figure 11. The recovery of $Fe_3O_4@SiO_2@IL-PMO/Pd$.

Received: 13 November 2021; Accepted: 25 April 2022
Published online: 13 May 2022

References

1. Azgomi, N. & Mokhtary, M. Nano-Fe3O4@ SiO2 supported ionic liquid as an efficient catalyst for the synthesis of 1, 3-thiazolidin-4-ones under solvent-free conditions. *J. Mol. Catal. A: Chem.* **398**, 58–64 (2015).
2. Cheng, T., Zhang, D., Li, H. & Liu, G. Magnetically recoverable nanoparticles as efficient catalysts for organic transformations in aqueous medium. *Green Chem.* **16**, 3401–3427 (2014).
3. Gawande, M. & Luque, R. *ChemCatChem* **6**, 3312–3313 (2014).
4. Gawande, M. B., Monga, Y., Zboril, R. & Sharma, R. K. *Coord. Chem. Rev.* **288**, 118–143 (2015).
5. Hui, C. *et al.* Core-shell Fe 3 O 4@ SiO 2 nanoparticles synthesized with well-dispersed hydrophilic Fe 3 O 4 seeds. *Nanoscale* **3**, 701–705 (2011).
6. Kango, S. *et al.* Surface modification of inorganic nanoparticles for development of organic–inorganic nanocomposites—A review. *Prog. Polym. Sci.* **38**, 1232–1261 (2013).
7. Reddy, L. H., Arias, J. L., Nicolas, J. & Couvreur, P. Magnetic nanoparticles: Design and characterization, toxicity and biocompatibility, pharmaceutical and biomedical applications. *Chem. Rev.* **112**, 5818–5878 (2012).
8. Shin, S. & Jang, J. Thiol containing polymer encapsulated magnetic nanoparticles as reusable and efficiently separable adsorbent for heavy metal ions. *Chem. Commun.* 4230–4232 (2007).
9. Dias, A., Hussain, A., Marcos, A. & Roque, A. A biotechnological perspective on the application of iron oxide magnetic colloids modified with polysaccharides. *Biotechnol. Adv.* **29**, 142–155 (2011).
10. Daniel-da-Silva, A. & Trindade, T. *Advances in Nanocomposite Technology* (Intech-Open Access Publisher, 2011).
11. Rossi, L. M., Costa, N. J., Silva, F. P. & Wojcieszak, R. Magnetic nanomaterials in catalysis: Advanced catalysts for magnetic separation and beyond. *Green Chem.* **16**, 2906–2933 (2014).
12. Du, Y. *et al.* Shell thickness-dependent microwave absorption of core–shell Fe3O4@ C composites. *ACS Appl. Mater. Interfaces.* **6**, 12997–13006 (2014).
13. Zhu, M., Meng, D., Wang, C. & Diao, G. Facile fabrication of hierarchically porous CuFe2O4 nanospheres with enhanced capacitance property. *ACS Appl. Mater. Interfaces.* **5**, 6030–6037 (2013).

14. Ahangaran, F., Hassanzadeh, A. & Nouri, S. Surface modification of Fe 3 O 4@ SiO 2 microsphere by silane coupling agent. *Int. Nano Lett.* **3**, 23 (2013).
15. Mirhosseini-Eshkevari, B., Ghasemzadeh, M. A. & Safaei-Ghomi, J. An efficient and green one-pot synthesis of indazolo [1, 2-b]-phthalazinetriones via three-component reaction of aldehydes, dimedone, and phthalhydrazide using Fe 3 O 4@ SiO 2 core–shell nanoparticles. *Res. Chem. Intermed.* **41**, 7703–7714 (2015).
16. Shailaja, J., Karthikeyan, S. & Ramamurthy, V. Cyclodextrin mediated solvent-free enantioselective photocyclization of N-alkyl pyridones. *Tetrahedron Lett.* **43**, 9335–9339 (2002).
17. Nagrik, D. M., Ambhore, D. & Gawande, M. B. One-pot preparation of β–amino carbonyl compounds by Mannich reaction using MgO/ZrO2 as effective and reusable catalyst. *Int. J. Chem.* **2**, 98–101 (2010).
18. Mirbagheri, R. & Elhamifar, D. Magnetic ethyl-based organosilica supported Schiff-base/indium: A very efficient and highly durable nanocatalyst. *J. Alloy. Compd.* **790**, 783–791 (2019).
19. Kargar, S., Elhamifar, D. & Zarnegaryan, A. Core–shell structured Fe3O4@ SiO2-supported IL/[Mo6O19]: A novel and magnetically recoverable nanocatalyst for the preparation of biologically active dihydropyrimidinones. *J. Phys. Chem. Solids* **146**, 109601 (2020).
20. Zebardasti, A., Dekamin, M. G., Doustkhah, E. & Assadi, M. H. N. Carbamate-isocyanurate-bridged periodic mesoporous organosilica for van der Waals CO2 capture. *Inorg. Chem.* **59**, 11223–11227 (2020).
21. Doustkhah, E. *et al.* Organosiloxane tunability in mesoporous organosilica and punctuated Pd nanoparticles growth; theory and experiment. *Microporous Mesoporous Mater.* **293**, 109832 (2020).
22. Doustkhah, E. & Ide, Y. Bursting exfoliation of a microporous layered silicate to three-dimensionally meso–microporous nanosheets for improved molecular recognition. *ACS Appl. Nano Mater.* **2**, 7513–7520 (2019).
23. Doustkhah, E. *et al.* Merging periodic mesoporous organosilica (PMO) with mesoporous aluminosilica (Al/Si-PMO): A catalyst for green oxidation. *Mol. Catal.* **482**, 110676 (2020).
24. Neysi, M., Zarnegaryan, A. & Elhamifar, D. Core–shell structured magnetic silica supported propylamine/molybdate complexes: An efficient and magnetically recoverable nanocatalyst. *New J. Chem.* **43**, 12283–12291 (2019).
25. Du, Q. *et al.* Immobilized palladium on surface-modified Fe3O4/SiO2 nanoparticles: As a magnetically separable and stable recyclable high-performance catalyst for Suzuki and Heck cross-coupling reactions. *Tetrahedron* **68**, 3577–3584 (2012).
26. Esmaeilpour, M. & Sardarian, A. R. Fe3O4@ SiO2/Schiff base complex of metal ions as an efficient and recyclable nanocatalyst for the green synthesis of quinoxaline derivatives. *Green Chem. Lett. Rev.* **7**, 301–308 (2014).
27. Deng, Y., Qi, D., Deng, C., Zhang, X. & Zhao, D. Superparamagnetic high-magnetization microspheres with an Fe3O4@ SiO2 core and perpendicularly aligned mesoporous SiO2 shell for removal of microcystins. *J. Am. Chem. Soc.* **130**, 28–29 (2008).
28. Rashid, J., Barakat, M., Ruzmanova, Y. & Chianese, A. Fe 3 O 4/SiO 2/TiO 2 nanoparticles for photocatalytic degradation of 2-chlorophenol in simulated wastewater. *Environ. Sci. Pollut. Res.* **22**, 3149–3157 (2015).
29. Gao, C. *et al.* A hierarchical meso-macroporous poly (ionic liquid) monolith derived from a single soft template. *Chem. Commun.* **51**, 4969–4972 (2015).
30. Li, J. *et al.* Pyrazinium polyoxometalate tetrakaidecahedron-like crystals esterify oleic acid with equimolar methanol at room temperature. *J. Catal.* **339**, 123–134 (2016).
31. Leng, Y., Zhao, J., Jiang, P. & Lu, D. POSS-derived solid acid catalysts with excellent hydrophobicity for highly efficient transformations of glycerol. *Catal. Sci. Technol.* **6**, 875–881 (2016).
32. Dai, Q., Wang, Y., Xu, W., Liu, Y. & Zhou, Y. Adsorption and specific recognition of DNA by using imprinted polymer layers grafted onto ionic liquid functionalized magnetic microspheres. *Microchim. Acta* **184**, 4433–4441 (2017).
33. Nasab, M. J. & Kiasat, A. R. Multifunctional Fe 3 O 4@ n SiO 2@ m SiO 2/Pr-Imi-NH 2· Ag core–shell microspheres as highly efficient catalysts in the aqueous reduction of nitroarenes: Improved catalytic activity and facile catalyst recovery. *RSC Adv.* **6**, 41871–41877 (2016).
34. Kong, Y., Tan, R., Zhao, L. & Yin, D. L-Proline supported on ionic liquid-modified magnetic nanoparticles as a highly efficient and reusable organocatalyst for direct asymmetric aldol reaction in water. *Green Chem.* **15**, 2422–2433 (2013).
35. Sadeghzadeh, S. M. A heteropolyacid-based ionic liquid immobilized onto magnetic fibrous nano-silica as robust and recyclable heterogeneous catalysts for the synthesis of tetrahydrodipyrazolopyridines in water. *RSC Adv.* **6**, 75973–75980 (2016).
36. Zolfigol, M. A., Ayazi-Nasrabadi, R., Baghery, S., Khakyzadeh, V. & Azizian, S. Applications of a novel nano magnetic catalyst in the synthesis of 1, 8-dioxo-octahydroxanthene and dihydropyrano [2, 3-c] pyrazole derivatives. *J. Mol. Catal. A: Chem.* **418**, 54–67 (2016).
37. Veisi, H., Sedrpoushan, A. & Hemmati, S. Palladium supported on diaminoglyoxime-functionalized Fe3O4 nanoparticles as a magnetically separable nanocatalyst in Heck coupling reaction. *Appl. Organomet. Chem.* **29**, 825–828 (2015).
38. Kaur, A. & Singh, V. Fe3O4@ SiO2@ Carbapalladacycle: A highly efficient and magnetically separable catalyst for C-C coupling reactions in ionic liquid media. *Chem. Lett.* **45**, 83–85 (2016).
39. Javidi, J. & Esmaeilpour, M. Fe3O4@ SiO2–imid–PMAn magnetic porous nanosphere as recyclable catalyst for the green synthesis of quinoxaline derivatives at room temperature and study of their antifungal activities. *Mater. Res. Bull.* **73**, 409–422 (2016).
40. Rathod, P. B. *et al.* Pd2+-loaded magnetic nanoassembly formed by magnetite nanoparticles crosslinked with Poly (acrylic acid) via amide bonds for Catalyzing Mizoroki-Heck coupling reaction. *ChemistrySelect* **3**, 8151–8158 (2018).
41. Hao, Y., ShengFu, J., XueFei, L., DanNi, Z. & Da, S. Magnetically recyclable Pd/gamma-AlOOH@ Fe3O4 catalysts and their catalytic performance for the Heck coupling reaction. *Sci. China-Chem.* **57**, 866–872 (2014).
42. Elhamifar, D., Mofatehnia, P. & Faal, M. Magnetic nanoparticles supported Schiff-base/copper complex: An efficient nanocatalyst for preparation of biologically active 3, 4-dihydropyrimidinones. *J. Colloid Interface Sci.* **504**, 268–275 (2017).
43. Elhamifar, D., Yari, O. & Karimi, B. Highly ordered mesoporous organosilica–titania with ionic liquid framework as very efficient nanocatalyst for green oxidation of alcohols. *J. Colloid Interface Sci.* **500**, 212–219 (2017).
44. Norouzi, M. & Elhamifar, D. Phenylene and isatin based bifunctional mesoporous organosilica supported schiff-base/manganese complex: an efficient and recoverable nanocatalyst. *Catal. Lett.* **149**, 619–628 (2019).

Author contributions
M.N. Investigation, Writing - original draft. D.E. Conceptualization, Writing - review & editing, Supervision, Visualization.

Competing interests
The authors declare no competing interests.

Additional information
Correspondence and requests for materials should be addressed to D.E.

Reprints and permissions information is available at www.nature.com/reprints.